1 **Stable carbon isotopes of dissolved inorganic carbon for a**

2 **zonal transect across the subpolar North Atlantic Ocean in**

3 **summer 2014**

4 **Matthew P. Humphreys[1], Florence M. Greatrix[1], Eithne Tynan[1],**

5 **Eric P. Achterberg[1,2], Alex M. Griffiths[3], Claudia H. Fry[1], Rebecca Garley[4],**

6 **Alison McDonald[5] and Adrian J. Boyce[5]**

7 [1]{Ocean and Earth Science, University of Southampton, Southampton, UK}

8 [2]{GEOMAR Helmholtz Centre for Ocean Research, Kiel, Germany}

9 [3]{Department of Earth Science and Engineering, Imperial College London, London, UK}

10 [4]{Bermuda Institute of Ocean Sciences, St George's, Bermuda}

11 [5]{Scottish Universities Environmental Research Centre, East Kilbride, UK}

12 Correspondence to: M. P. Humphreys (m.p.humphreys@soton.ac.uk)

13

14 **Abstract**

15 The stable carbon isotope composition of dissolved inorganic carbon ($\delta^{13}C_{DIC}$) in seawater

16 was measured in samples collected during June—July 2014 in the subpolar North Atlantic.

17 Sample collection was carried out on the RRS *James Clark Ross* cruise JR302, part of the

18 'Radiatively Active Gases from the North Atlantic Region and Climate Change'

19 (RAGNARoCC) research programme. The observed $\delta^{13}C_{DIC}$ values for cruise JR302 fall in a

20 range from -0.07 ‰ to +1.95 ‰, relative to the Vienna Peedee Belemnite standard. From

21 duplicate samples collected during the cruise, the 1σ precision for the 341 results is 0.08 ‰,

22 which is similar to our previous work and other studies of this kind. We also performed a

23 cross-over analysis using nearby historical $\delta^{13}C_{DIC}$ data, which indicated that there were no

24 significant systematic offsets between our measurements and previously published results.

25 We also included seawater reference material (RM) produced by A. G. Dickson (Scripps

26 Institution of Oceanography, USA) in every batch of analysis, enabling us to improve upon

27 the calibration and quality-control procedures from a previous study. The $\delta^{13}C_{DIC}$ is consistent

28 within each RM batch, although its value is not certified. We report $\delta^{13}C_{DIC}$ values of

1   1.15 ± 0.03 ‰ and 1.27 ± 0.05 ‰ for batches 141 and 144 respectively. Our JR302 $\delta^{13}C_{DIC}$

2   data can be used – along with measurements of other biogeochemical variables – to constrain

3   the processes that control DIC in the interior ocean, in particular the oceanic uptake of

4   anthropogenic carbon dioxide and the biological carbon pump. Our $\delta^{13}C_{DIC}$ results are

5   available from the British Oceanographic Data Centre – doi:10.5285/22235f1a-b7f3-687f-

6   e053-6c86abc0c8a6.

7

8   **1   Introduction**

9   The global ocean has absorbed up to half of the anthropogenic carbon dioxide (CO_2) emitted

10   since the early 1800s (Sabine et al., 2004; Khatiwala et al., 2009, 2013) and it continues to

11   take up about a quarter of annual CO_2 emissions at the present day (Le Quéré et al., 2009),

12   substantially decreasing CO_2 accumulation in the atmosphere. The consequences of this

13   uptake include a decline in pH – known as ocean acidification – with lower pH values

14   predicted to persist for centuries longer than the atmospheric CO_2 anomaly (Caldeira and

15   Wickett, 2003), which will have impacts on marine biogeochemistry and ecology that we are

16   only just beginning to understand (Doney et al., 2009; Achterberg, 2014; Gaylord et al.,

17   2015).

18   In order to predict the response of the oceanic CO_2 sink to the continuing rise of the

19   atmospheric partial pressure of CO_2 ($p$$CO_2$), it is useful to first understand the existing spatial

20   distribution of anthropogenic dissolved inorganic carbon (DIC_{anth}) in the ocean interior.

21   Various methods have been employed to this end (Sabine and Tanhua, 2010), including back-

22   calculation from DIC, total alkalinity (TA) and dissolved oxygen observations (Brewer, 1978;

23   Chen and Millero, 1979; Gruber et al., 1996); inference from the oceanic distributions of

24   other anthropogenic gases such as chlorofluorocarbons (Hall et al., 2002; Waugh et al., 2006);

25   and multi-linear regressions using measurements from pairs of cruises in the same region, but

26   separated in time (Friis et al., 2005; Tanhua et al., 2007). Oceanic measurements during the

27   past few decades (Quay et al., 2007) and over longer timescales in ice cores (Rubino et al.,

28   2013) show that the rise in $p$$CO_2$ and DIC has been accompanied by a decline in the carbon-

29   13 content of DIC, relative to carbon-12 (reported as $\delta^{13}C$, Eqs. 1 and 2), a phenomenon

30   called the 'Suess effect' (Keeling, 1979). This is caused by the lower $\delta^{13}C$ of anthropogenic

31   CO_2 relative to pre-industrial and present-day atmospheric CO_2, and it provides another

32   approach to constrain the spatial distribution and inventory of anthropogenic DIC (e.g. Quay

1   et al., 1992, 2003, 2007; Sonnerup et al., 1999, 2007; Körtzinger et al., 2003). The Suess

2   effect has caused significant changes in the present-day distribution of $\delta^{13}C_{DIC}$ in the ocean

3   interior (Olsen and Ninnemann, 2010). Continued observations of oceanic $\delta^{13}C_{DIC}$ are

4   essential for verification of the parameterisations of ocean carbon cycle models (Sonnerup

5   and Quay, 2012).

6   Here, we present measurements of $\delta^{13}C_{DIC}$ from a zonal transect across the subpolar North

7   Atlantic Ocean in June—July 2014. The cruise, JR302 on the RRS *James Clark Ross*, was

8   carried out as part of the 'Radiatively Active Gases from the North Atlantic Region and

9   Climate Change' (RAGNARoCC) research programme. Our observations fill important

10   spatiotemporal gaps in the existing global dataset (Schmittner et al., 2013), and will contribute

11   towards the scientific objectives summarised above. Our analysis was carried out following

12   the methodology presented by Humphreys et al. (2015a), but we have been able to make

13   several improvements to the raw data processing and calibration procedures by inclusion of

14   seawater reference material (RM) in every batch of sample analysis. This RM, produced by

15   A. G. Dickson (Scripps Institution of Oceanography, USA), is mainly used for assessing the

16   accuracy of non-isotopic marine carbonate chemistry measurements, and it does not have a

17   certified $\delta^{13}C_{DIC}$ value. Nevertheless, the $\delta^{13}C_{DIC}$ of different RM bottles from the same RM

18   batch should be consistent, allowing us to assess the consistency of our measurements

19   between analysis batches. We determine $\delta^{13}C_{DIC}$ values for the two RM batches that we

20   measured (141 and 144), which could be used to check for systematic offsets between our

21   results and those from other laboratories. We also use the RM results to carry out a statistical

22   analysis of our measurement precision both within and between analysis batches.

23

2   Sample collection

2.1   Cruise details

26   The $\delta^{13}C_{DIC}$ samples were collected during RRS *James Clark Ross* cruise JR302, which was

27   an approximately zonal transect from St John's, Newfoundland, Canada to Immingham, UK

28   (Fig. 1), from June—July 2014 (King and Holliday, 2015). During the crossing, several

29   transects were sailed in towards the coast of Greenland, and in the eastern region the ship

30   carried out a short meridional transect north towards Iceland in order to sample the Extended

31   Ellett Line (Holliday and Cunningham, 2013).

2.2 Sample collection and storage

Prior to sample collection, the containers were thoroughly rinsed with deionised water (MilliQ water, Millipore, >18.2 mΩ cm^{-1}). Samples were collected from the source (either seawater sampling bottle or underway seawater supply) via silicone tubing, following established best-practice protocols (Dickson et al., 2007; McNichol et al., 2010), as summarised here. The containers were thoroughly rinsed with excess seawater sample immediately before filling until overflowing with seawater, taking care not to generate or trap air bubbles. Two different sample containers were used: (1) 100 ml glass 'bottles' with ground glass stoppers, lubricated with Apiezon® L grease, and held shut with electrical tape; (2) 50 ml glass 'vials', with plastic screw-cap lids and PTFE/silicone septa. In order to sterilise each sample, 0.02 % of the sample container volume of saturated mercuric chloride solution was added before sealing. A 1 ml air headspace (i.e. 1 % of the sample volume) was also introduced to the bottles, prior to poisoning, by removing this volume of seawater via pipette. This prevents thermal expansion/contraction of the seawater from breaking the air-tight seal. However, the flexible septa on the vials allowed them to be sealed when full of seawater. All samples were stored in the dark until analysis.

3 Sample analysis

All of the $\delta^{13}C_{DIC}$ samples were analysed at the Scottish Universities Environmental Research Centre Isotope Community Support Facility (SUERC-ICSF) in East Kilbride (UK), in June—July 2015. We describe the analysis procedure here only in brief, as it was identical to that of Humphreys et al. (2015a).

The samples were analysed in 13 batches. Each analysis batch consisted of up to 88 measurements, 16 of which were of calibration standards, and the remainder were of seawater samples, 'blanks' or RM (Fig. 2). Each batch underwent a three-step process of overgassing, equilibration and measurement. For the overgassing step, the air in each of the measurement vials (12 ml Exetainer®) was flushed out and replaced with helium by a PAL system (CTC Analytics). For equilibration, the standards, samples and RM were reacted with phosphoric acid to convert all DIC to CO_2. Finally, the gaseous headspace in each measurement vial was then sampled by the PAL system and transferred to a Thermo Scientific Delta V mass spectrometer via a Thermo Scientific Gasbench 2, and was measured 10 times (called technical replicates).

1   For seawater samples and RM, 4 drops of concentrated phosphoric acid were added to the

2   Exetainer analysis vials prior to overgassing, and 1 ml of liquid sample was then injected into

3   each vial for equilibration. For the standards, only the solid powder standard was added to the

4   analysis vials prior to overgassing, and 1 ml of dilute (10 % by volume) phosphoric acid was

5   added to each vial for equilibration. During batches 4 and 6—13, 'blanks' were prepared in

6   the same way as the standards, except that the Exetainer analysis vials were completely empty

7   for overgassing, and had the same dilute acid added as the standards in that batch.

8

9   ## 4 Measurement processing

10   We were able to make improvements to the processing of the raw measurements from our

11   previous study (Humphreys et al., 2015a), in part by using the results from the RM that were

12   included in every batch. The processing sequence used in this study is described in full here,

13   including parts that are the same as in Humphreys et al. (2015a); differences between the two

14   approaches are then discussed later. All processing was carried out using MATLAB®

15   (MathWorks, USA).

16   ### 4.1 Definitions

17   The relative abundance of ^{13}C to ^{12}C in a sample X is given by Eq. 1. The R_X is then

18   normalised to a reference standard – i.e. V-PDB (Coplen, 1995) – using Eq. 2.

19    $$R_X = \frac{[^{13}C]_X}{[^{12}C]_X} \qquad (1)$$

20   where $[^{13}C]_X$ and $[^{12}C]_X$ are the concentrations of ^{13}C and ^{12}C respectively in X.

21    $$\delta^{13}C = \frac{R_{sample} - R_{V\text{-}PDB}}{R_{V\text{-}PDB}} \times 1000\ ‰ \qquad (2)$$

22   ### 4.2 General procedure

23   #### 4.2.1 Anomalous measurement removal

24   Anomalous $\delta^{13}C$ measurements were first removed from the sets of technical replicates. These

25   typically occurred when the CO_2 concentration in a replicate was too low, causing the peak

26   area to fall outside the calibrated range. Thus all measurements with a peak area less than

1   5 mV s were judged to be anomalous and discarded, and if this applied to 5 or more of the

2   original 10 technical replicates for a given sample, the entire sample was discarded.

4.2.2 Peak area (linearity) correction

4   Virtually all samples, standards and RM showed a consistent decline in both peak area and

5   raw $\delta^{13}C$ through each set of technical replicates, called 'linearity' (Fig. 3). To correct for this,

6   we first 'normalised' the peak area and raw $\delta^{13}C$ of each set of technical replicates by

7   subtracting the mean peak area and $\delta^{13}C$ respectively from each replicate; every set of

8   technical replicates thus had a mean normalised peak area and $\delta^{13}C$ of 0 (mV s or ‰,

9   respectively). We then performed an ordinary least-squares linear regression of normalised

10    $\delta^{13}C$ against normalised peak area using all technical replicates from all of the samples,

11   standards and RM. The regression was forced through the origin and had a gradient (L) of

12   0.0147 ‰ (mV s)$^{-1}$. This was used to make a 'peak area correction' to all technical replicates:

13    $$\delta_{lin} = \delta_{raw} - L(a - A_{lin}) \tag{3}$$

14   where δ_{lin} is the linearity-corrected $\delta^{13}C$, δ_{raw} is the raw $\delta^{13}C$ measurement, L is the correction

15   gradient (i.e. 0.0147 ‰ (mV s)$^{-1}$), a is the peak area for the technical replicate in mV s, and

16   A_{lin} is 20 mV s – the peak area that the correction is made to. The value of A_{lin} was chosen

17   because it is the mean peak area for all of the seawater samples, thus minimising the

18   magnitude of this correction.

4.2.3 Averaging

20   After the peak area correction had been applied, the mean $\delta^{13}C$ of each set of technical

21   replicates was calculated. These mean values were then used for the remainder of the data

22   processing.

4.2.4 Blank correction

24   A 'blank correction' was then applied to the standards only (MAB, NA and CA). This was

25   necessary because phosphoric was added to these after the overgassing step, so any CO_2

26   dissolved in the acid would be included in the measurement. It was not necessary for the

27   seawater samples and RM, because here the acid was added prior to overgassing. The

28   different procedures were necessary because of the different states of the standards and

29   samples (solid and liquid, respectively).

1   A pair of 'blank' measurements were included during analysis batches 4 and 6—13. These

2   were clean, empty Exetainer analysis vials that were otherwise treated in the same way as the

3   standards: acid had been added after overgassing. The mean ± standard deviation (SD) peak

4   area and linearity-corrected δ^{13}C of all of these blanks were 0.277 ± 0.024 mV s and 19.42 ±

5   2.47 ‰ respectively. These mean values were then used to make the blank correction to all

6   standards:

7    $$\delta_{blank} = \frac{a\delta_{lin} - A_{blank}D_{blank}}{a - A_{blank}} \qquad (4)$$

8   where δ_{blank} is the blank-corrected δ^{13}C, and A_{blank} and D_{blank} are the mean blank peak area and

9   δ^{13}C (i.e. 0.277 ± 0.024 mV s and 19.42 ± 2.47 ‰, respectively).

10   Even after this blank correction, there remained unexplained relationships between peak area

11   and δ^{13}C for the standards (Fig. 4). We therefore performed an ordinary least-squares

12   regression between peak area and blank-corrected δ^{13}C for all measurements in all analysis

13   batches of each standard, and took the value of the regression line at a peak area of 20 mV s

14   as the δ^{13}C value for that standard in order to generate the V-PDB calibration curve (Table 1).

15   ### 4.2.5 Calibration to V-PDB

16   A second-order polynomial fit was generated to determine the certified δ^{13}C values for the

17   standards (Table 1) from their blank-corrected mean values (Fig. 5):

18   $$\delta_{cert} = c\delta_{blank}^2 + s\delta_{blank} + f \qquad (5)$$

19   where δ_{cert} is the certified δ^{13}C value (Table 1); and c, s and f are coefficients describing the

20   curvature, stretch and offset respectively of the calibration fit, taking the following values: $c =$

21   -4.321×10^{-3} ‰$^{-1}$, $s = 1.189$, $f = -36.563$ ‰. Equation 5 was then used to calibrate all of the

22   sample and RM measurements, by inputting the linearity-corrected δ^{13}C values as δ_{blank}; the

23   output (δ_{cert}) gives the final, calibrated δ^{13}C$_{DIC}$, relative to the V-PDB international standard

24   (Coplen, 1995).

4.3 Quality control

4.3.1 Practical problems

We have excluded $\delta^{13}C_{DIC}$ results from our dataset where practical problems were encountered and noted during sample analysis that discredited specific measurements. For example, during analysis batch 9 the automated needle became detached part way through the overgassing step, resulting in the loss of measurements after this point. The measurements that have been excluded in this way can be identified as gaps in Fig. 2.

4.3.2 Cross-over analysis

A cross-over analysis was performed using XOVER v1.0.0.1 (Humphreys, 2015) in order to evaluate the consistency of this study's results with 'historical' measurements from the Schmittner et al. (2013) $\delta^{13}C_{DIC}$ compilation and our previous study (Humphreys et al., 2014a, 2014b, 2015a). The XOVER program follows a similar procedure to the secondary quality control toolbox of Lauvset and Tanhua (2015). Firstly, all historical sampling stations within 150 km of a JR302 CTD station were selected. The 150 km distance is the best compromise for minimising the spatial offset between the JR302 and historical observations while still capturing enough historical data to perform an effective cross-over analysis. At each of these historical stations, a piecewise cubic Hermite interpolating polynomial (PCHIP) fit was generated to predict $\delta^{13}C_{DIC}$ from depth. Values of $\delta^{13}C_{DIC}$ at depths which were equivalent to the JR302 observations were then interpolated using these PCHIP fits. Only JR302 data from deeper than 200 m were used, in order to limit the effect of seasonal variability in $\delta^{13}C_{DIC}$, which is relatively high near the ocean surface due to biological processes. The differences between the JR302 and historical $\delta^{13}C_{DIC}$ values were calculated and combined into a mean ± SD value for each cruise in the historical datasets.

4.4 Precision from duplicates

The SD obtained if one sample was measured many times (i.e. 1σ precision, 68.3 % confidence interval) can also be estimated from many duplicate measurements of different samples: it is equal to the mean of the absolute differences between the duplicate pairs divided by $2/\sqrt{\pi}$ (Thompson and Howarth, 1973; Humphreys et al., 2015a), as follows. For this purpose, each pair of duplicate measurements of a sample i is considered to be two values ($d_{i,1}$ and $d_{i,2}$) that have been randomly selected from a normal distribution with a SD equal to

1 the 1σ measurement precision (P) and a mean equal to the 'true' $\delta^{13}C_{DIC}$ value for that

2 sample. The 'duplicate pair difference' (D) for the sample i is then calculated by subtracting

3 the $\delta^{13}C_{DIC}$ of the first duplicate from that of the second (i.e. $D_i = d_{i,2} - d_{i,1}$). As P is the same

4 for every sample, D is normally distributed with a mean of 0 and a SD of $P\sqrt{2}$. The 1σ

5 precision P can thus be estimated from the SD of all D by dividing it by $\sqrt{2}$. Alternatively: the

6 absolute values of D follow a half-normal distribution, which has a mean value $2P/\sqrt{\pi}$, thus P

7 can also be estimated from the mean of the duplicate pair absolute differences (i.e. the mean

8 of all $|D|$) by dividing the latter by $2/\sqrt{\pi}$. This last calculation (Eq. 6) was carried out for all of

9 the analytical duplicate pairs and separately for the sampling duplicates to determine their

10 respective 1σ confidence intervals:

11 $$P = \frac{\sqrt{\pi}}{2N} \sum_{i=1}^{N} |D_i| \qquad (6)$$

12 where N is the total number of duplicate pairs.

13

14 ## 5   Results and discussion

15 ### 5.1   Dataset availability

16 The $\delta^{13}C_{DIC}$ measurements described in this study are publicly available, free-of-charge from

17 the British Oceanographic Data Centre, with doi: 10.5285/22235f1a-b7f3-687f-e053-

18 6c86abc0c8a6 (Humphreys et al., 2015b). The data will also be submitted to the Carbon

19 Dioxide Information Analysis Centre (CDIAC, Oak Ridge National Laboratory, USA) along

20 with other carbonate chemistry and macronutrient metadata from cruise JR302 once those

21 become available.

22 ### 5.2   Results in context

23 #### 5.2.1   Interior $\delta^{13}C_{DIC}$ distribution

24 Our final $\delta^{13}C_{DIC}$ results are presented in Figs. 6—8. To first order, $\delta^{13}C_{DIC}$ is highest in

25 surface waters (shallower than c. 40 m) taking values up to 2 ‰. Then, $\delta^{13}C_{DIC}$ decreases with

26 depth to minima just below 0 ‰ at about 500 m, before increasing again to intermediate

27 values of around 1 ‰ in deeper waters. This pattern is in general agreement with previous

28 studies (Schmittner et al., 2013).

1 ## 5.2.2 Cross-over analysis

2 The cross-over analysis compared the results from this study with 3 nearby historical cruises:

3 OACES93, 58GS20030922 and D379 (Table 2). The mean $\delta^{13}C_{DIC}$ residual was significantly

4 different from 0 for all of these cruises ($p < 0.01$). Despite this, the mean ($\pm$ SD) $\delta^{13}C_{DIC}$

5 residuals for OACES93 and D379 (-0.08 $\pm$ 0.14 ‰ and +0.08 $\pm$ 0.16 ‰ respectively) were no

6 larger than our reported measurement precision of 0.08 ‰. Although the mean ($\pm$ SD)

7 residual for 58GS20030922 was greater (-0.19 $\pm$ 0.16 ‰), it must firstly be considered that

8 this depends on only 3 matching $\delta^{13}C_{DIC}$ measurements, and secondly that it is still within the

9 range of the accuracy of 0.1—0.2 ‰ reported for its parent dataset (Schmittner et al., 2013).

10 We therefore conclude that any systematic bias between the results of this study and existing

11 $\delta^{13}C_{DIC}$ datasets is negligible relative to the uncertainties of the measurements themselves.

12 ## 5.3 Measurement uncertainty

13 ### 5.3.1 Sample container types

14 In tests of duplicate samples collected in these two different container types, Humphreys et al.

15 (2015a) were unable to find evidence of any systematic offset between $\delta^{13}C_{DIC}$ measurements

16 from the same two sample container types that were used in this study. Here, 5 pairs of

17 sampling duplicates were collected with one sample in each container type. The mean $\pm$ SD

18 difference in $\delta^{13}C_{DIC}$ for these duplicate pairs was -0.01 $\pm$ 0.04 ‰, with the difference always

19 calculated as the $\delta^{13}C_{DIC}$ value measured in the sample collected in a 50 ml vial subtracted

20 from that collected in a 250 ml bottle. A one-sample t-test could not reject the null hypothesis

21 that this mean difference in $\delta^{13}C_{DIC}$ was equal to 0 ($p = 0.63$). We therefore conclude that the

22 container type does not cause a systematic offset in the $\delta^{13}C_{DIC}$ measurement, in agreement

23 with Humphreys et al. (2015a).

24 ### 5.3.2 Seawater samples

25 The typical precision for seawater $\delta^{13}C_{DIC}$ measurements is in the range from about 0.03 ‰ to

26 0.23 ‰ (Olsen et al., 2006; Quay et al., 2007; McNichol et al., 2010; Griffith et al., 2012),

27 and we previously reported a value of 0.10 ‰ based on sampling duplicates (Humphreys et

28 al., 2015a). In this study, we again determined the precision of the seawater sample

29 measurements from both analytical and sampling duplicates. There were 341 analytical

30 duplicate pairs, which had a mean absolute difference of 0.075 ‰ and therefore a 1σ precision

1   of 0.067 ‰, and 36 sampling duplicate pairs, with a mean absolute difference of 0.090 ‰ and

2   therefore a 1σ precision of 0.080 ‰. Although the latter is slightly greater, indicating that the

3   sample collection and storage procedures might have adversely affected the measurement

4   precision, Levene's test (Levene, 1960) carried out on the (non-absolute) duplicate differences

5   could not reject the null hypothesis that the analytical and sampling precisions are in fact the

6   same ($p = 0.33$). We therefore report the higher value of 0.08 ‰ as the 1σ precision for this

7   dataset; it falls within the range of other studies of this kind. It is important to note that this

8   value is based on consecutively-analysed samples, and so might not reflect additional

9   uncertainty engendered by samples being measured non-consecutively or in different analysis

10   batches. However, it is shown in the following section that any such additional uncertainty

11   was negligible.

12   ### 5.3.3 Seawater reference material

13   Two 'batches' of RM were measured in this study: 141 and 144

14   (http://cdiac.ornl.gov/oceans/Dickson_CRM/batches.html). Each batch consists of multiple

15   bottles of virtually identical seawater. Bottles from within each batch will henceforth be

16   referred to as RM141 and RM144 respectively. The RM are primarily intended for assessment

17   of the accuracy of marine carbonate chemistry measurements, in particular DIC and TA

18   (Dickson et al., 2003); they are sterilised and sealed in air-tight bottles such that the DIC and

19   TA are consistent in all RM bottles within each RM batch, and so these variables are stable

20   and do not change on timescales of up to a few years. Although the $\delta^{13}C_{DIC}$ value is unknown

21   for these RM, the nature of the preparation and storage process means that we can assume that

22   it is also consistent within each RM batch (A. G. Dickson 2015, pers. comm., 18 June), thus

23   allowing us to assess the relative accuracy of our $\delta^{13}C_{DIC}$ measurements between different

24   analysis batches. Unpublished past measurements of $\delta^{13}C_{DIC}$ in similar RM (batches 17, 18

25   and 19) have supported this assumption, with the $\delta^{13}C_{DIC}$ in multiple (i.e. 3—9) bottles from

26   the same RM batch found to have a SD of about 0.01 ‰ (A. G. Dickson 2015, pers. comm.,

27   18 June).

28   Typically, we made 6 measurements of each RM bottle, all within the same analysis batch.

29   These were also spread throughout the analysis batch, and hence not consecutive (Fig. 2). The

30   SD of these results for each bottle therefore represents a longer-term precision estimate than

31   that which we get from the analytical duplicates, which were always analysed one

32   immediately after the other. This approach therefore indicates the reproducibility of

1   measurements carried out anywhere within a single analysis batch (rather than just

2   consecutively). The 1σ precision from the analytical duplicates was 0.067 ‰, while the

3   average SD of the measurements within each RM bottle was slightly smaller (0.058 ‰). This

4   indicates that the position of samples within each analysis batch did not influence the $\delta^{13}C_{DIC}$

5   measurement; the relative accuracy of two consecutive measurements is no better than that

6   between measurements from opposite ends of an analysis batch.

7   The next step is to verify that the difference in $\delta^{13}C_{DIC}$ between different RM bottles of the

8   same batch is negligible. During analysis batch 13, we measured 6 different RM144 bottles,

9   each up to 6 times (Table 3). The mean of the 6 measurements for each RM bottle was taken

10   as its $\delta^{13}C_{DIC}$ value. The SD of these 6 mean values was 0.028 ‰. Next, we compared this to

11   measurements of different RM bottles across different analysis batches. One RM144 bottle

12   was measured during each of analysis batches 1—12. The mean value was calculated for each

13   analysis batch, and the SD of these 12 mean values was 0.056 ‰. Although larger than the

14   SD for the 6 RM bottles within batch 13, this value is still smaller than the overall

15   measurement precision based on samples within the same batch. In addition, we used

16   Levene's test (Levene, 1960) for the null hypothesis that the SD of the 6 RM bottles in

17   analysis batch 13 was the same as the SD of the 12 RM bottles in analysis batches 1—12; the

18   resulting p-value of 0.14 was too great to confidently reject the null hypothesis, so we cannot

19   be certain that there truly is greater variance between analysis batches than within them.

20   Our final $\delta^{13}C_{DIC}$ values are: +1.15 ‰ for RM141, and +1.27 ‰ for RM144 (Table 3).

21   ### 5.3.4 Calibration standards

22   The precision of measurements of the calibration standards was greater (i.e. worse) than that

23   of the samples and RM; all calibrated MAB, NA and CA measurements had SDs of 0.13 ‰,

24   0.46 ‰, and 0.35 ‰ respectively, compared with about 0.08 ‰ for the RM (Fig. 9). We

25   suggest that this is a result of the necessarily different practical treatment of the liquid

26   seawater samples and RM compared with the powdered solid standards. The former were

27   added to concentrated acid that had been overgassed with helium, while the latter were

28   themselves overgassed prior to addition of dilute acid that may have contained some CO_2.

29   The blank correction should have corrected for the influence of this CO_2, but there remained

30   an unexplained relationship between peak area and raw $\delta^{13}C$ for the standards even after its

31   application (Fig. 4). The poor precision for the standards might be associated with the very

1 small quantities (0.1—1.1 mg) that were measured out into the Exetainer analysis vials, in

2 contrast to the 1 ml of seawater sample or RM that was used each time – the former would be

3 more susceptible to contamination. This result provides a strong incentive to develop seawater

4 RM with a certified $\delta^{13}C_{DIC}$ value, which can be analysed following the exact same method as

5 the samples during future studies of this kind.

6 **5.4 Changes from our previous study**

7 There were 3 main changes to the data processing from our previous study (Humphreys et al.,

8 2015a): the peak area correction, which previously was carried out using a different

9 relationship for the seawater samples and for each standard; the V-PDB calibration, which

10 was previously carried out separately for each analysis batch; and the drift correction, which

11 is absent in the current study.

12 5.4.1 Peak area (linearity) correction

13 The linearity correction in this study was different from that in our previous work

14 (Humphreys et al., 2015a), because we did not find the same relationships between peak area

15 and $\delta^{13}C$. This was due to hardware changes to the mass spectrometer in the intervening time

16 between the studies. We therefore believe that the linearity correction used in each study was

17 appropriate, and would recommend determining the best way to apply this correction on a

18 case-by-case basis for different datasets. Another result of these hardware changes was a

19 reduction in the mean peak area for the seawater samples from about 35 mV s to about

20 20 mV s. There is no evidence of any adverse (or particularly beneficial) effects on the quality

21 of the results of either study as a result of these modifications.

22 5.4.2 The V-PDB calibration

23 The V-PDB calibration in this study was a single equation determined from all of the

24 measurements of all of the calibration standards in every analysis batch, where previously we

25 determined a separate equation for each batch (Humphreys et al., 2015a). This new approach

26 delivered significantly better RM results between batches, as a result of the relatively high

27 uncertainty in the measurements of the calibration standards; the apparent differences in

28 calibration equations between analysis batches were in fact an artefact of these uncertainties.

29 The consequence of this for our previous study is a decrease in precision, but it does not

30 constitute a systematic error. If we apply a different calibration to each batch, as in our

1   previous study, we find mean ± SD across all analysis batches of the mean $\delta^{13}C_{DIC}$ of each

2   RM within each batch for RM141 (4 RM bottles across 4 batches) and RM144 (18 RM bottles

3   across 13 batches) of 1.19 ± 0.08 ‰ and 1.30 ± 0.11 ‰ respectively; by way of comparison,

4   our new approach in this study yields 1.15 ± 0.03 ‰ and 1.26 ± 0.05 ‰ respectively. To

5   determine the significance of these apparent differences, we took the mean RM141 and

6   RM144 results for each analysis batch and used them to test two different null hypotheses,

7   separately for each RM and calibration method. Firstly, we used Welch's unequal variances *t*-

8   test (Welch, 1947) for the null hypothesis that the mean $\delta^{13}C_{DIC}$ across all batches was the

9   same regardless of the V-PDB calibration method. For both RM141 and RM144, the null

10   hypothesis could not be rejected at the 5 % significance level, with *p*-values of 0.47 and 0.28

11   respectively. Secondly, we used Levene's test (Levene, 1960) for the null hypothesis that the

12   variance of these batch mean results was the same regardless of the V-PDB calibration

13   method. For both RM141 and RM144, the null hypothesis was rejected at the 5 %

14   significance level, with *p*-values of 0.01 and 0.03 respectively. Thus we conclude that the

15   change to the V-PDB calibration method – using a single equation across all analysis batches,

16   instead of a separate one for each – results in an improvement in the precision of results from

17   different analysis batches (i.e. reduced SD), and that it does not cause a systematic bias in

18   these results (i.e. no change in the mean).

19   This result cannot necessarily be applied to recalibrate the results of our previous study, as no

20   RM measurements were carried out then. In this study, all measurements were carried out on

21   consecutive days over a 5-week period. However, in the previous study, there were gaps of

22   several weeks between some analysis batches, and there is no way to objectively assess the

23   consistency of the calibration over these breaks retrospectively. Therefore, although the

24   uncertainty estimate for the previous study was probably too generous and should be

25   approximately doubled, there is no evidence of a systematic bias.

26   Additionally, the form of the equation used to carry out the V-PDB calibration (Eq. 5) is a

27   second-order polynomial in this study, which differs from the circle used by Humphreys et al.

28   (2015a). This change makes virtually no difference to the final $\delta^{13}C_{DIC}$ results, but it provides

29   a calibration equation that only gives one possible corrected value for each input $\delta^{13}C$. The

30   calibration equation used in this study is also much easier to interpret, with coefficients

31   directly corresponding to the curvature (*c*), stretch (*s*) and translational offset (*f*) of the curve.

1   5.4.3 Drift correction

2   No drift correction was performed during this study, while Humphreys et al. (2015a) used the

3   measurements of pairs standards at the middle and end of each analysis batch to correct for

4   instrumental drift. However, the RM measurements spaced throughout each analysis batch in

5   the present study indicated that no drift correction was required, sometimes in disagreement

6   with the calibration standards (Fig. 10). We suggest that this apparent conflict is again a result

7   of the significantly greater uncertainty in individual measurements of the calibration standards

8   relative to those of seawater samples and RM.

9   As for the V-PDB calibration, this difference does not cause an important systematic offset to

10 the results from our previous study, but rather an increase in the variance. To support this

11 claim, we applied a drift correction following Humphreys et al. (2015a) to our RM144 results

12 in analysis batches 1—8 and 10—12. Analysis batches 9 and 13 were excluded due to the

13 lack of RM data and the different arrangement of RM respectively (Fig. 2). The mean ± SD of

14 all individual RM144 measurements (i.e. up to 6 per RM bottle) was 1.26 ± 0.08 ‰ with no

15 drift correction, but 1.22 ± 0.17 ‰ when a drift correction was applied. We used Levene's test

16 (Levene, 1960) to confidently reject the null hypothesis that the SDs were equal with and

17 without the drift correction ($p = 0.0001$), thus the decline in precision caused by applying the

18 drift correction was significant. We also used Welch's unequal variances t-test (Welch, 1947)

19 for the null hypothesis that the mean value of these RM144 measurements were the same with

20 and without drift correction; although the null hypothesis could be tentatively rejected at the

21 5 % significance level ($p = 0.048$) the actual magnitude of the difference in the mean values

22 (c. 0.04 ‰) is smaller than the measurement precision of either study, and can therefore be

23 considered negligible.

24 However, for the same reasons as given regarding the V-PDB calibration, it would not be

25 appropriate to recommend retrospective changes to the results of our previous study in the

26 absence of any RM measurements therein.

27

28 **6   Conclusions**

29 We successfully measured $\delta^{13}C_{DIC}$ in 341 samples collected from June—July 2014 during

30 RRS *James Clark Ross* cruise JR302 in the subpolar North Atlantic Ocean. The $\delta^{13}C_{DIC}$

31 values were in the range from -0.07 ‰ to +1.95 ‰ relative to V-PDB and had a 1σ

1 uncertainty of 0.08 ‰. Our results are internally consistent, with no systematic offsets

2 between or within analysis batches, and a cross-over analysis revealed no systematic bias

3 relative to nearby historical data in deep waters. We have also established $\delta^{13}C_{DIC}$ values for

4 batches 141 (+1.15 ‰) and 144 (+1.27 ‰) of seawater RM obtained from A. G. Dickson

5 (Scripps Institute of Oceanography, USA), and demonstrated that RM bottles within the same

6 batch have consistent $\delta^{13}C_{DIC}$ values. These RM greatly enhanced our ability to quantitatively

7 assess and improve our data processing approach, and lead us to conclude that the

8 development of an internationally-available seawater RM with a certified $\delta^{13}C_{DIC}$ value would

9 be a valuable boon to future measurements of this kind.

10

Author contributions

12 E. Tynan determined the sampling strategy, and E. Tynan, A. M. Griffiths, C. H. Fry and R.

13 Garley collected the samples. F. M. Greatrix, A. McDonald and M. P. Humphreys carried out

14 the measurements and data processing. M. P. Humphreys wrote the manuscript with

15 contributions from all co-authors.

16

Acknowledgements

23

24

1 **References**

2 Achterberg, E. P.: Grand challenges in marine biogeochemistry, Front. Mar. Sci., 1, 7,

3 doi:10.3389/fmars.2014.00007, 2014.

4 Brewer, P. G.: Direct observation of the oceanic CO_2 increase, Geophys. Res. Lett., 5(12),

5 997–1000, doi:10.1029/GL005i012p00997, 1978.

6 Caldeira, K. and Wickett, M. E.: Anthropogenic carbon and ocean pH, Nature, 425(6956),

7 365–365, doi:10.1038/425365a, 2003.

8 Chen, G.-T. and Millero, F. J.: Gradual increase of oceanic CO_2, Nature, 277(5693), 205–206,

9 doi:10.1038/277205a0, 1979.

10 Coplen, T. B.: Reporting of stable hydrogen, carbon, and oxygen isotopic abundances,

11 Geothermics, 24(5–6), 707–712, doi:10.1016/0375-6505(95)00024-0, 1995.

12 Dickson, A. G., Afghan, J. D. and Anderson, G. C.: Reference materials for oceanic CO_2

13 analysis: a method for the certification of total alkalinity, Mar. Chem., 80(2–3), 185–197,

14 doi:10.1016/S0304-4203(02)00133-0, 2003.

15 Dickson, A. G., Sabine, C. L. and Christian, J. R.: Guide to best practices for ocean CO_2

16 measurements, PICES Special Publication 3., 2007.

17 Doney, S. C., Fabry, V. J., Feely, R. A. and Kleypas, J. A.: Ocean Acidification: The Other

18 CO_2 Problem, Annu. Rev. Marine Sci., 1, 169–192,

19 doi:10.1146/annurev.marine.010908.163834, 2009.

20 Friis, K., Körtzinger, A., Pätsch, J. and Wallace, D. W. R.: On the temporal increase of

21 anthropogenic CO_2 in the subpolar North Atlantic, Deep-Sea Res. Pt I, 52(5), 681–698,

22 doi:10.1016/j.dsr.2004.11.017, 2005.

23 Gaylord, B., Kroeker, K. J., Sunday, J. M., Anderson, K. M., Barry, J. P., Brown, N. E.,

24 Connell, S. D., Dupont, S., Fabricius, K. E., Hall-Spencer, J. M., Klinger, T., Milazzo, M.,

25 Munday, P. L., Russell, B. D., Sanford, E., Schreiber, S. J., Thiyagarajan, V., Vaughan, M. L.

26 H., Widdicombe, S. and Harley, C. D. G.: Ocean acidification through the lens of ecological

27 theory, Ecology, 96(1), 3–15, doi:10.1890/14-0802.1, 2015.

28 Griffith, D. R., McNichol, A. P., Xu, L., McLaughlin, F. A., Macdonald, R. W., Brown, K. A.

29 and Eglinton, T. I.: Carbon dynamics in the western Arctic Ocean: insights from full-depth

1   carbon isotope profiles of DIC, DOC, and POC, Biogeosciences, 9(3), 1217–1224,
2   doi:10.5194/bg-9-1217-2012, 2012.

3   Gruber, N., Sarmiento, J. L. and Stocker, T. F.: An improved method for detecting
4   anthropogenic CO_2 in the oceans, Global Biogeochem. Cy., 10(4), 809–837,
5   doi:10.1029/96GB01608, 1996.

6   Hall, T. M., Haine, T. W. N. and Waugh, D. W.: Inferring the concentration of anthropogenic
7   carbon in the ocean from tracers, Global Biogeochem. Cy., 16(4), 1131,
8   doi:10.1029/2001GB001835, 2002.

9   Holliday, N. P. and Cunningham, S.: The Extended Ellett Line: Discoveries from 65 years of
10   marine observations west of the UK, Oceanography, 26(2), 156–163,
11   doi:10.5670/oceanog.2013.17, 2013.

12   Humphreys, M. P.: Cross-over analysis of hydrographic variables: XOVER v1.0, Ocean and
13   Earth Science, University of Southampton, UK., pp 8, doi:10.13140/RG.2.1.1629.0405, 2015.

14   Humphreys, M. P., Achterberg, E. P., Griffiths, A. M., McDonald, A. and Boyce, A. J.: Ellett
15   Line measurements of stable isotope composition of dissolved inorganic carbon in the
16   Northeastern Atlantic and Nordic Seas during summer 2012, British Oceanographic Data
17   Centre, Natural Environment Research Council, UK, doi:10/xph, 2014a.

18   Humphreys, M. P., Achterberg, E. P., Griffiths, A. M., McDonald, A. and Boyce, A. J.:
19   UKOA measurements of the stable isotope composition of dissolved inorganic carbon in the
20   Northeastern Atlantic and Nordic Seas during summer 2012, British Oceanographic Data
21   Centre, Natural Environment Research Council, UK, doi:10/xpj, 2014b.

22   Humphreys, M. P., Achterberg, E. P., Griffiths, A. M., McDonald, A. and Boyce, A. J.:
23   Measurements of the stable carbon isotope composition of dissolved inorganic carbon in the
24   northeastern Atlantic and Nordic Seas during summer 2012, Earth Syst. Sci. Data, 7, 127–
25   135, doi:10.5194/essd-7-127-2015, 2015a.

26   Humphreys, M. P., Greatrix, F. M., Tynan, E., Griffiths, A. M., Fry, C. H., Garley, R.,
27   Achterberg, E. P., McDonald, A. and Boyce, A. J.: Stable carbon isotopes of dissolved
28   inorganic carbon for RRS *James Clark Ross* cruise JR302 in the subpolar North Atlantic
29   Ocean from June to July 2014, British Oceanographic Data Centre, Natural Environment
30   Research Council, UK, doi:10.5285/22235f1a-b7f3-687f-e053-6c86abc0c8a6, 2015b.

1 Keeling, C. D.: The Suess effect: ^{13}Carbon-^{14}Carbon interrelations, Environ. Int., 2(4–6),

2 229–300, doi:10.1016/0160-4120(79)90005-9, 1979.

3 Khatiwala, S., Primeau, F. and Hall, T.: Reconstruction of the history of anthropogenic CO_2

4 concentrations in the ocean, Nature, 462(7271), 346–349, doi:10.1038/nature08526, 2009.

5 Khatiwala, S., Tanhua, T., Mikaloff Fletcher, S., Gerber, M., Doney, S. C., Graven, H. D.,

6 Gruber, N., McKinley, G. A., Murata, A., Ríos, A. F. and Sabine, C. L.: Global ocean storage

7 of anthropogenic carbon, Biogeosciences, 10(4), 2169–2191, doi:10.5194/bg-10-2169-2013,

8 2013.

9 King, B. A. and Holliday, N. P.: JR302 Cruise Report, The 2014 RAGNARoCC, OSNAP and

10 Extended Ellett Line cruise, National Oceanography Centre, Southampton, UK, pp. 76, 2015.

11 Körtzinger, A., Quay, P. D. and Sonnerup, R. E.: Relationship between anthropogenic CO_2

12 and the ^{13}C Suess effect in the North Atlantic Ocean, Global Biogeochem. Cy., 17(1), 5–1–5–

13 20, doi:10.1029/2001GB001427, 2003.

14 Lauvset, S. K. and Tanhua, T.: A toolbox for secondary quality control on ocean chemistry

15 and hydrographic data, Limnol. Oceanogr. Methods, doi:10.1002/lom3.10050, 2015.

16 Le Quéré, C., Raupach, M. R., Canadell, J. G., Marland, G., Bopp, L., Ciais, P., Conway, T.

17 J., Doney, S. C., Feely, R. A., Foster, P., Friedlingstein, P., Gurney, K., Houghton, R. A.,

18 House, J. I., Huntingford, C., Levy, P. E., Lomas, M. R., Majkut, J., Metzl, N., Ometto, J. P.,

19 Peters, G. P., Prentice, I. C., Randerson, J. T., Running, S. W., Sarmiento, J. L., Schuster, U.,

20 Sitch, S., Takahashi, T., Viovy, N., van der Werf, G. R. and Woodward, F. I.: Trends in the

21 sources and sinks of carbon dioxide, Nature Geosci., 2(12), 831–836, doi:10.1038/ngeo689,

22 2009.

23 Levene, H.: Robust tests for equality of variances, in Contributions to Probability and

24 Statistics: Essays in Honor of Harold Hotelling, pp. 278–292, Stanford University Press,

25 USA., 1960.

26 McNichol, A., Quay, P. D., Gagnon, A. R. and Burton, J. R.: Collection and measurement of

27 carbon isotopes in seawater DIC, in The GO-SHIP Repeat Hydrography Manual: A

28 Collection of Expert Reports and Guidelines, IOCCP Report No. 14, ICPO Publication Series

29 No. 134, Version 1., 2010.

1   Olsen, A. and Ninnemann, U.: Large δ^{13}C Gradients in the Preindustrial North Atlantic

2   Revealed, Science, 330(6004), 658–659, doi:10.1126/science.1193769, 2010.

3   Olsen, A., Omar, A. M., Bellerby, R. G. J., Johannessen, T., Ninnemann, U., Brown, K. R.,

4   Olsson, K. A., Olafsson, J., Nondal, G., Kivimäe, C., Kringstad, S., Neill, C. and Olafsdottir,

5   S.: Magnitude and origin of the anthropogenic CO_2 increase and ^{13}C Suess effect in the

6   Nordic seas since 1981, Global Biogeochem. Cy., 20(3), GB3027,

7   doi:10.1029/2005GB002669, 2006.

8   Quay, P., Sonnerup, R., Westby, T., Stutsman, J. and McNichol, A.: Changes in the ^{13}C/^{12}C of

9   dissolved inorganic carbon in the ocean as a tracer of anthropogenic CO_2 uptake, Global

10   Biogeochem. Cy., 17, GB1004, doi:10.1029/2001GB001817, 2003.

11   Quay, P. D., Tilbrook, B. and Wong, C. S.: Oceanic Uptake of Fossil Fuel CO_2: Carbon-13

12   Evidence, Science, 256(5053), 74 –79, doi:10.1126/science.256.5053.74, 1992.

13   Quay, P. D., Sonnerup, R., Stutsman, J., Maurer, J., Körtzinger, A., Padin, X. A. and

14   Robinson, C.: Anthropogenic CO_2 accumulation rates in the North Atlantic Ocean from

15   changes in the ^{13}C/^{12}C of dissolved inorganic carbon, Global Biogeochem. Cy., 21, GB1009,

16   doi:10.1029/2006GB002761, 2007.

17   Rubino, M., Etheridge, D. M., Trudinger, C. M., Allison, C. E., Battle, M. O., Langenfelds, R.

18   L., Steele, L. P., Curran, M., Bender, M., White, J. W. C., Jenk, T. M., Blunier, T. and

19   Francey, R. J.: A revised 1000 year atmospheric δ^{13}C-CO_2 record from Law Dome and South

20   Pole, Antarctica, J. Geophys. Res. Atmos., 118(15), 8482–8499, doi:10.1002/jgrd.50668,

21   2013.

22   Sabine, C. L. and Tanhua, T.: Estimation of Anthropogenic CO_2 Inventories in the Ocean,

23   Annu. Rev. Marine Sci., 2, 175–198, doi:10.1146/annurev-marine-120308-080947, 2010.

24   Sabine, C. L., Feely, R. A., Gruber, N., Key, R. M., Lee, K., Bullister, J. L., Wanninkhof, R.,

25   Wong, C. S., Wallace, D. W. R., Tilbrook, B., Millero, F. J., Peng, T.-H., Kozyr, A., Ono, T.

26   and Rios, A. F.: The Oceanic Sink for Anthropogenic CO_2, Science, 305(5682), 367–371,

27   doi:10.1126/science.1097403, 2004.

28   Schmittner, A., Gruber, N., Mix, A. C., Key, R. M., Tagliabue, A. and Westberry, T. K.:

29   Biology and air–sea gas exchange controls on the distribution of carbon isotope ratios (δ^{13}C)

30   in the ocean, Biogeosciences, 10(9), 5793–5816, doi:10.5194/bg-10-5793-2013, 2013.

1   Sonnerup, R. E. and Quay, P. D.: ^{13}C constraints on ocean carbon cycle models, Global

2   Biogeochem. Cy., 26(2), GB2014, doi:10.1029/2010GB003980, 2012.

3   Sonnerup, R. E., Quay, P. D., McNichol, A. P., Bullister, J. L., Westby, T. A. and Anderson,

4   H. L.: Reconstructing the oceanic ^{13}C Suess Effect, Global Biogeochem. Cy., 13(4), 857–872,

5   doi:10.1029/1999GB900027, 1999.

6   Sonnerup, R. E., McNichol, A. P., Quay, P. D., Gammon, R. H., Bullister, J. L., Sabine, C. L.

7   and Slater, R. D.: Anthropogenic δ^{13}C changes in the North Pacific Ocean reconstructed using

8   a multiparameter mixing approach (MIX), Tellus B, 59(2), 303–317, doi:10.1111/j.1600-

9   0889.2007.00250.x, 2007.

10   Tanhua, T., Körtzinger, A., Friis, K., Waugh, D. W. and Wallace, D. W. R.: An estimate of

11   anthropogenic CO_2 inventory from decadal changes in oceanic carbon content, Proc. Natl.

12   Acad. Sci. U.S.A., 104(9), 3037 –3042, doi:10.1073/pnas.0606574104, 2007.

13   Thompson, M. and Howarth, R. J.: The rapid estimation and control of precision by duplicate

14   determinations, Analyst, 98(1164), 153–160, doi:10.1039/AN9739800153, 1973.

15   Waugh, D. W., Hall, T. M., McNeil, B. I., Key, R. and Matear, R. J.: Anthropogenic CO_2 in

16   the oceans estimated using transit time distributions, Tellus B, 58(5), 376–389,

17   doi:10.1111/j.1600-0889.2006.00222.x, 2006.

18   Welch, B. L.: The Generalization of Student's Problem When Several Different Population

19   Variances Are Involved, Biometrika, 34(1-2), 28–35, doi:10.1093/biomet/34.1-2.28, 1947.

20

21

1   Table 1. The SUERC-ICSF calibration standards.

Name	Chemical composition	Certified $\delta^{13}C$ (V-PDB) / ‰	Blank-corrected $\delta^{13}C$ at 20 mV s / ‰
MAB	$CaCO_3$	+2.48	+38.13
NA	$NaHCO_3$	–4.67	+30.13
CA	$CaCO_3$	–24.23	+10.80

2

3

1   Table 2. Results of the cross-over analysis. Sources: OACES93 on R/V *Malcolm Baldrige*,

2   carbon PIs F. Millero, R. Feely and P. Quay, data from Schmittner et al. (2013);

3   58GS20030922 on G. O. *Sars*, carbon PIs A. Olsen and T. Johannessen, data from Schmittner

4   et al. (2013); D379 on RRS *Discovery*, carbon PI A. M. Griffiths, data from Humphreys et al.

5   (2015a).

Cross-over cruise	Sampling date	Mean of $\delta^{13}C_{DIC}$ residuals / ‰	SD of $\delta^{13}C_{DIC}$ residuals / ‰	Number of residuals
OACES93	Aug 1993	-0.08	0.14	19
58GS20030922	Oct 2003	-0.19	0.16	3
D379	Aug 2012	0.08	0.16	253

6

7

Earth System
Science
Data

Open Access

Discussions

1   Table 3. Results of the RM measurements. The RM mean and standard deviation (SD)

2   columns contain the mean and SD of the replicate values in each row, except for the rows

3   marked 'All', which contain the mean and SD of all the RM mean values for each RM batch.

RM batch	RM bottle	Analysis batch	Replicate RM $\delta^{13}C_{DIC}$ measurements / ‰						RM mean / ‰	RM SD / ‰
141	585	1	1.03	1.10	1.09	1.10	1.21	1.13	1.11	0.06
141	764	3	1.21	1.17	1.11	1.16	0.98	1.20	1.14	0.09
141	455	8	1.21	1.13	1.20	1.22	1.19	1.14	1.18	0.04
141	526	12	1.17	1.19	1.25	1.17	1.15	1.14	1.18	0.04
141	All	All							1.15	0.03
144	30	1	1.20	1.14	1.25	1.19	1.28	1.21	1.21	0.05
144	1079	2	1.20	1.22	1.32	1.28	1.27	1.12	1.24	0.07
144	1141	3	1.36	1.24	1.30	1.32	1.23	1.29	1.29	0.05
144	1024	4	1.27	1.30	1.34	1.36	1.24	1.23	1.29	0.05
144	461	5	1.29	1.24	1.18				1.24	0.05
144	516	6	1.19	1.29	1.28	1.19	1.25	1.28	1.25	0.04
144	399	7	1.44	1.26	1.35	1.35	1.27	1.31	1.33	0.06
144	1017	8	1.12	1.16	1.10	1.07	1.18	1.10	1.12	0.04
144	950	9	1.31	1.29					1.30	0.01
144	90	10	1.27	1.33	1.36				1.32	0.04
144	881	11	1.21	1.25	1.32	1.4	1.26		1.29	0.07
144	822	12	1.31	1.28	1.13	1.32	1.30		1.27	0.08
144	151	13	1.36	1.34	1.36	1.34	1.23		1.33	0.05
144	339	13	1.12	1.30	1.25	1.29	1.36	1.30	1.27	0.08
144	575	13	1.29	1.27	1.23	1.36	1.27		1.28	0.05
144	636	13	1.24	1.22	1.33	1.34	1.26		1.28	0.05
144	703	13	1.17	1.29	1.25	1.33	1.30		1.27	0.06
144	745	13	1.30	1.33	1.26	1.21	1.12		1.24	0.08
144	All	All							1.27	0.05

4

5

1
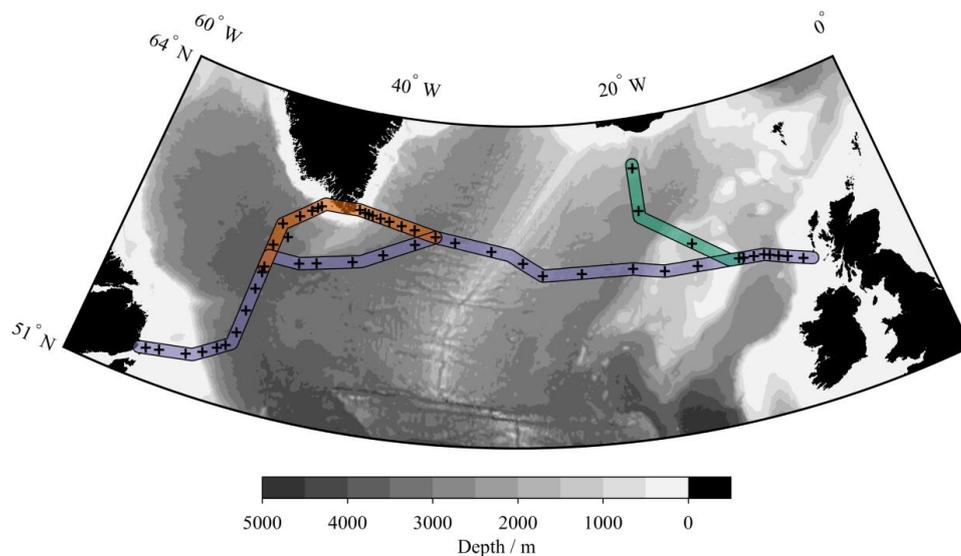
Figure 1. Bathymetric map of the subpolar North Atlantic Ocean. Black plusses show $\delta^{13}C_{DIC}$ sampling locations during cruise JR302. Coloured sections indicate illustrated transects: blue for Fig. 6, orange for Fig. 7, green for Fig. 8. Bathymetry data are from the GEBCO_2014 grid, version 20150318, http://www.gebco.net.
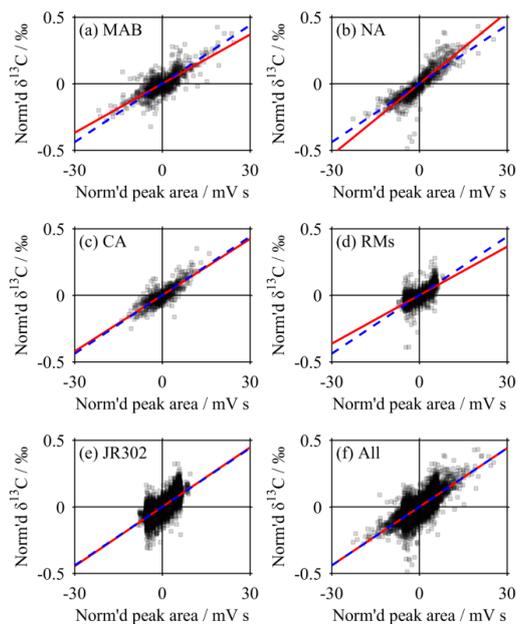
6
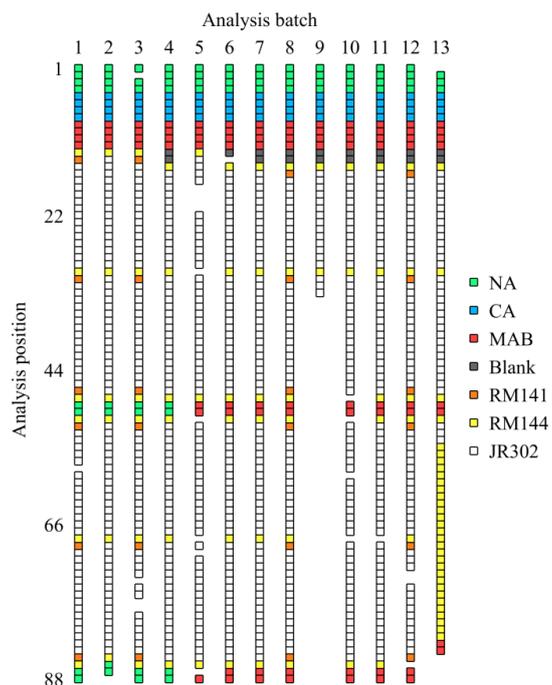
1

2   Figure 2. Schematic arrangement of calibration standards (NA, CA and MAB), blanks, RM

3   and samples (JR302) within each analysis batch. Each square represents a separate

4   measurement (i.e. a set of 10 technical replicates). Gaps are left where results have failed

5   quality control.

6

7

1

Figure 3. The peak area correction relationship. All technical replicates are plotted, normalised such that the mean peak area and $\delta^{13}C$ for each set of technical replicates are both 0 (‰ or mV s respectively). Red line is the same in each plot, showing the mean relationship used for all of the peak area corrections, while each dashed blue line shows the equivalent relationship determined only from the data scattered in each panel. Individual data points are semi-transparent.

8

1
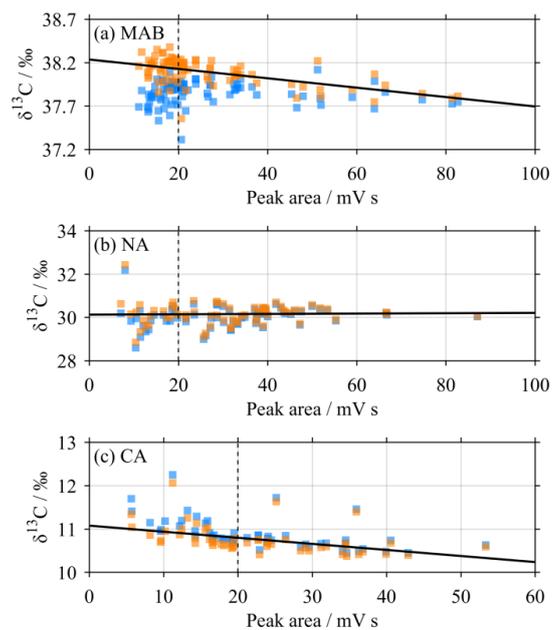
Figure 4. The blank correction for the standards. Each panel shows relationships between peak area and $\delta^{13}C$ for (a) MAB, (b) NA and (c) CA before (blue) and after (orange) blank correction. The solid black lines are linear least-squares regressions for the data after blank correction. Their intercepts with the dashed black lines at 20 mV s were used as the mean values for each standard to generate the V-PDB calibration curve (Fig. 5). Note that the panels have different axes resolutions.
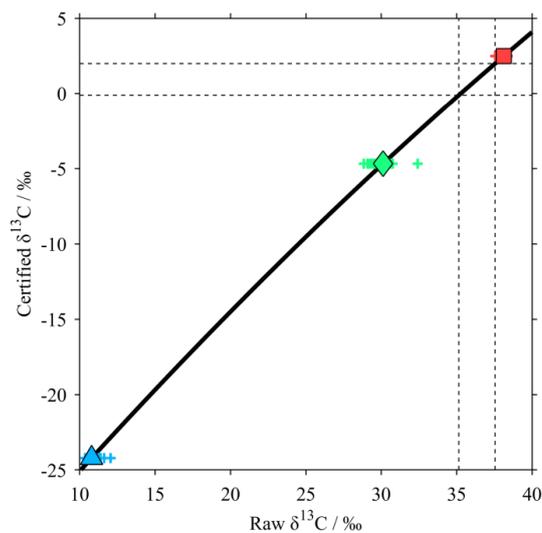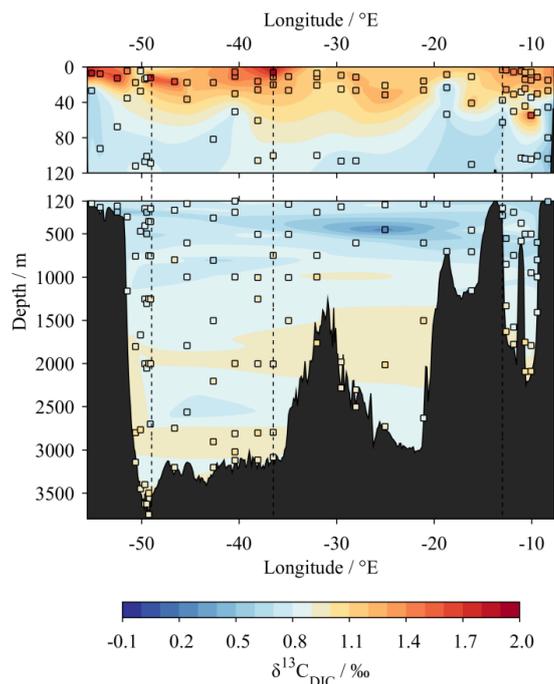
1

2   Figure 5. The V-PDB calibration. Mean values for each standard: red square for MAB, green

3   diamond for NA, blue triangle for CA; results of individual measurements of standards shown

4   as plusses in the same colours as the means. Thick black line shows the calibration curve (Eq.

5   5); dashed black lines enclose the range of δ^{13}C values for the seawater samples and RM.

6

Figure 6. Zonal section of $\delta^{13}C_{DIC}$ results from this study, from west to east across the subpolar North Atlantic Ocean (blue in Fig. 1). Coloured squares show actual sample locations and $\delta^{13}C_{DIC}$ values. Vertical dashed lines indicate locations of joints with edges of Figs. 7 and 8. Bathymetry data are from the GEBCO_2014 grid, version 20150318, http://www.gebco.net.

1
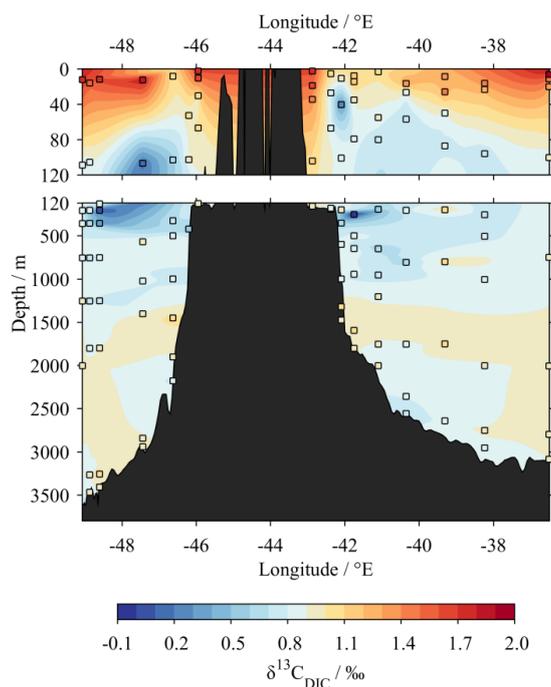
Figure 7. Zonal section of $\delta^{13}C_{DIC}$ results from this study, from west to east near southern Greenland (orange in Fig. 1). Coloured squares show actual sample locations and $\delta^{13}C_{DIC}$ values. Bathymetry data are from the GEBCO_2014 grid, version 20150318, http://www.gebco.net.
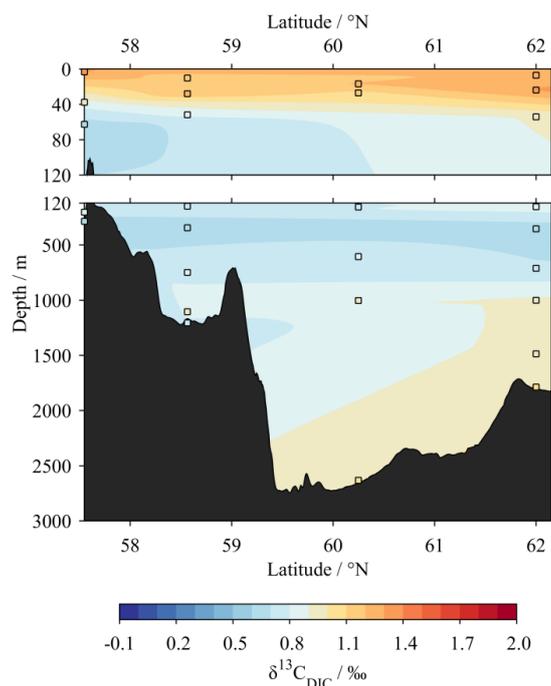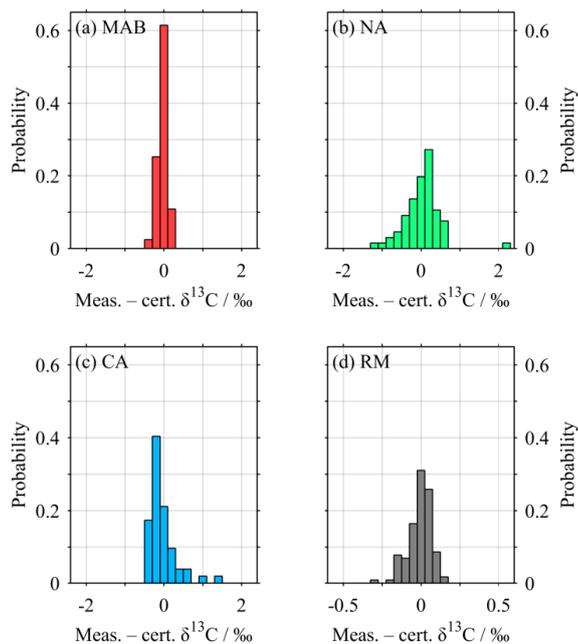
Figure 8. Meridional section of $\delta^{13}C_{DIC}$ results from this study, from south to north in the eastern subpolar North Atlantic Ocean (green in Fig. 1). Coloured squares show actual sample locations and $\delta^{13}C_{DIC}$ values. Bathymetry data are from the GEBCO_2014 grid, version 20150318, http://www.gebco.net.
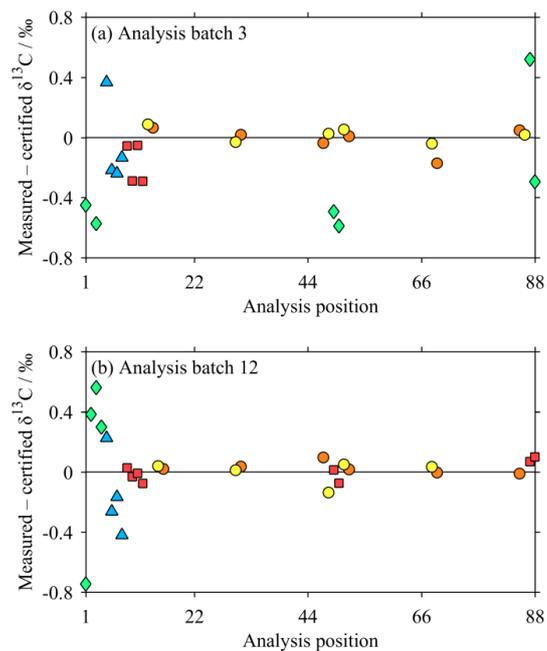
1

Figure 9. Histograms of offset of all standards and RM from their certified values (Table 1).

Mean ± SD are: (a) MAB, -0.03 ± 0.13 ‰; (b) NA, +0.02 ± 0.46 ‰; (c) CA, -0.04 ± 0.35 ‰;

and (d) all RM, -0.01 ± 0.08 ‰. 'Certified' values for RM are our final values, 1.15 ‰ for

RM141 and 1.27 ‰ for RM144 (Table 3). Note the increased horizontal resolution in (d).

Earth System
Science
Data

Open Access

Discussions

1

2   Figure 10. Examples of results of standards and RM within batches (a) 3 and (b) 12. Red

3   squares for MAB, green diamonds for NA, blue triangles for CA, orange circles for RM141,

4   yellow circles for RM144.

5